THE PHOTOCHEMICAL REFLECTANCE INDEX FROM DIRECTIONAL CORNFIELD REFLECTANCES: OBSERVATIONS AND SIMULATIONS

[Research Paper]

Yen-Ben Cheng[1,*], Elizabeth M. Middleton[2], Qingyuan Zhang[3], Lawrence A. Corp[4], Jonathan Dandois[5], and William P. Kustas[6,a]

[1]Earth Resources Technology, Inc., Laurel, MD 20707, USA

[2]Biospheric Sciences Laboratory, National Aeronautics and Space Administration/Goddard Space Flight Center, Greenbelt, MD 20771, USA

[3]Unversities Space Research Association, Columbia, MD 21044, USA

[4]Sigma Space Corporation, Lanham, MD 20706, USA

[5]Department of Geography and Environmental Systems, University of Maryland Baltimore County, Baltimore, MD 21250, USA

[6]Hydrology and Remote Sensing Laboratory, USDA Agricultural Research Service, Beltsville, MD 20705, USA

*Corresponding author:

Code 618, NASA Goddard Space Flight Center, Greenbelt, MD 20771, USA

Tel: +1 (301) 614-6636; Fax: +1 (301) 614-6695

Email: Yen-Ben.Cheng@nasa.gov

[a]USDA is an equal opportunity provider and employer

ABSTRACT

The two-layer Markov chain Analytical Canopy Reflectance Model (ACRM) was linked with *in situ* hyperspectral leaf optical properties to simulate the Photochemical Reflectance Index (PRI) for a corn crop canopy at three different growth stages. This is an extended study after a successful demonstration of PRI simulations for a cornfield previously conducted at an early vegetative growth stage. Consistent with previous *in situ* studies, sunlit leaves exhibited lower PRI values than shaded leaves. Since sunlit (shaded) foliage dominates the canopy in the reflectance hotspot (coldspot), the canopy PRI derived from field hyperspectral observations displayed sensitivity to both view zenith angle and relative azimuth angle at all growth stages. Consequently, sunlit and shaded canopy sectors were most differentiated when viewed along the azimuth matching the solar principal plane. These directional PRI responses associated with sunlit/shaded foliage were successfully reproduced by the ACRM. As before, the simulated PRI values from the current study were closer to *in situ* values when both sunlit and shaded leaves were utilized as model input data in a two-layer mode, instead of a one-layer mode with sunlit leaves only. Model performance as judged by correlation between *in situ* and simulated values was strongest for the mature corn crop ($r = 0.87$, RMSE = 0.0048), followed by the early vegetative stage ($r = 0.78$; RMSE = 0.0051) and the early senescent stage ($r = 0.65$; RMSE = 0.0104). Since the benefit of including shaded leaves in the scheme varied across different growth stages, a further analysis was conducted to investigate how variable fractions of sunlit/shaded leaves affect the canopy PRI values expected for a cornfield, with implications for remote sensing monitoring options. Simulations of the sunlit to shaded canopy ratio near 50/50 ± 10 (e.g., 60/40) matching field observations at all growth stages were examined. Our results

suggest in the importance of the sunlit/shaded fraction and canopy structure in understanding and interpreting PRI.

Highlights:

- Demonstrating PRI responses to illumination conditions and viewing geometry at leaf and canopy level.
- Validating the capability of the two-layer Analytical Canopy Reflectance Model for PRI simulations in a cornfield at different growth stages.
- Investigating how canopy structure associated with variable fraction of sunlit/shaded leaves affect the PRI values.

Keywords: hyperspectral, two-layer Analytical Canopy Reflectance Model (ACRM), photochemical reflectance index (PRI), cornfield

1. INTRODUCTION

Remotely sensed spectral bio-indicators have the potential to play a critical role in monitoring and modeling processes in time and space for our Earth's ecosystems, including the exchange of carbon between the biosphere and the atmosphere. This is because uncertainties exist in how ecosystems will function and what feedbacks to expect, especially under disturbances induced by the changing climate (Garbulsky et al., 2011; Middleton et al., 2011). One of the widely used concepts to model carbon assimilation by plants is the light use efficiency (LUE) model (Monteith, 1972; Monteith, 1977). This approach describes carbon assimilation, in the form of gross or net primary productivity (GPP, NPP), as the product of the absorbed photosynthetically active radiation (APAR) and LUE. Previous studies have shown that LUE can vary based on vegetation type, environmental conditions, and temporal resolution of the observations (Anderson et al., 2000; Garbulsky et al., 2011; Gower et al., 1999; King et al., 2011; Middleton et al., 2011; Peñuelas et al., 2011).

The importance of accurate LUE estimation has been emphasized in recent studies (e.g., (Lin et al., 2011; Peñuelas et al., 2011), reporting that errors in LUE are a major contributor to biases in annual carbon assimilation estimates. Current tools and methods developed for LUE estimation usually utilize a look-up table of maximum possible LUE, which is then downscaled by an adjustment coefficient determined using meteorological data (e.g., air temperature and VPD) to account for non-optimal environmental effects (Law and Waring, 1994; Mahadevan et al., 2008; Prince and Goward, 1995; Xiao et al., 2004). This approach is used for the satellite data product available from the Terra and Aqua Moderate Resolution Imaging Spectroradiometers (MODIS), the MOD17 GPP product (Heinsch et al., 2003; Heinsch et al., 2006). However, with this approach, errors are usually introduced into LUE estimates due to

uncertainties about the fixed values within the look-up table and the meteorological data used for scaling factors. Moreover, these meteorological data usually have a much larger footprint than the area of interest, and hence, are not always representative for local LUE (Middleton et al., 2011). On the other hand, a spectral bio-indicator directly derived from vegetation optical properties has been shown capable of providing useful estimates of LUE without needing ancillary information or relying on meteorological data (Garbulsky et al., 2011; Hall et al., 2011; Huemmrich et al., 2009; Middleton et al., 2009; Middleton et al., 2011; Peñuelas et al., 2011).

The LUE of plants is closely linked to the reversible photoprotective responses of the foliar xanthophyll pigment cycle to illumination conditions, especially as induced by saturating mid-day irradiances. These responses are expressed by a spectral bio-indicator, the Photochemical Reflectance Index (PRI; (Gamon et al., 1990; Gamon et al., 1992; Gamon et al., 1997; Peñuelas et al., 1995). This PRI information can be used to model the down-regulation of photosynthesis (Demmig-Adams and Adams III, 1996). The PRI utilizes a narrow physiologically active green band centered at 531 nm and a reference band most typically centered at 570 nm, in the form of a normalized difference index (i.e., [ρ531-ρ570]/[ρ531+ρ570]). The PRI has been increasingly used and examined for its correlation with LUE across various vegetation types and scales (Cheng et al., 2009; Coops et al., 2010; Filella et al., 1996; Gamon et al., 1993; Gamon et al., 1992; Gamon et al., 1997; Garbulsky et al., 2011; Garbulsky et al., 2008; Hall et al., 2011, 2012; Hilker et al., 2011; Hilker et al., 2012; Inoue et al., 2008; Middleton et al., 2009; Middleton et al., 2011; Nichol et al., 2002; Peñuelas et al., 1995; Peñuelas and Inoue, 2000; Peñuelas et al., 1997).

However, studies have also shown that various factors affect the remote sensing-based PRI:LUE relationship at canopy or ecosystem scales, including viewing geometry, canopy

structure, leaf area index (LAI), soil background, pigment content and shadow fraction (Barton and North, 2001; Cheng et al., 2009; Drolet et al., 2005; Gamon et al., 2001; Hall et al., 2008; Hernández-Clemente et al., 2011; Hilker et al., 2008a; Hilker et al., 2008b; Middleton et al., 2009; Nichol and Grace, 2010; Sims and Gamon, 2002; Sims et al., 2006; Stylinski et al., 2002). Furthermore, previous studies have also shown the importance of taking both sunlit and shaded foliage into account to explain PRI behaviors at the canopy level, since sunlit foliage is more likely to experience high light-induced environmental stress, and to have lower LUE, and hence, lower PRI values (Cheng et al., 2009; Cheng et al., 2010; Hall et al., 2008; Hilker et al., 2008b; Middleton et al., 2009; Peñuelas et al., 1995). It follows that we must have more understanding about the relative roles of sunlit and shaded foliage in canopies, and associated canopy structure, to improve our knowledge regarding PRI:LUE relationships. Radiative Transfer (RT) models provide a powerful tool to study this topic since they are designed to quantitatively examine changes in vegetation optical properties with leaf biochemical and canopy biophysical properties (Cheng et al., 2006; Jacquemoud et al., 1996; Verhoef, 1984; Zarco-Tejada et al., 2003; Zhang et al., 2011).

Canopy PRI was studied for water stress detection using the PROSPECT leaf model linked with the SAILh and FLIGHT canopy RT models to produce a non-stressed version of the PRI in two tree-structured orchards and a maize field (Suárez et al., 2009). In a more recent study, the leaf model LIBERTY was coupled with the canopy model INFORM to study PRI as a physiological stress indicator in conifer forests (Hernández-Clemente et al., 2011). Both studies focused on PRI acquired at near nadir angles. Cheng et al. (2010) utilized *in situ* leaf optical properties coupled with a Markov chain Analytical two-layer Canopy Reflectance Model (ACRM; (Kuusk, 1995a, b, 2001) to simulate nadir and directional PRI at the canopy level in a

106 cornfield, which was compared and validated with *in situ* canopy PRI observations. That study
107 showed that ACRM successfully simulated PRI under various viewing geometries for a corn
108 crop in the early vegetative stage without noticeable environmental stressors present, and
109 explored how several canopy structure parameters affected PRI values. The ACRM-simulated
110 PRI showed the best agreement with *in situ* values when the model was run in a two layer
111 simulation mode, using leaf optical properties from sunlit leaves as the upper layer and shaded
112 leaves as the lower canopy (Cheng et al., 2010). In the current study, we took a step further to
113 examine the robustness of the same algorithm to simulate PRI through three different growth
114 stages for a corn crop, examining early vegetative, fully mature, and senescent canopies. Our
115 objective was to determine whether the directional PRI responses previously observed for a
116 young, vigorous canopy also continue to be present throughout the growing season, and to
117 characterize and evaluate them. We also investigated how the vertical distribution of sunlit and
118 shaded leaves affect an important structure-related variable, the canopy sunlit/shaded foliage
119 ratio, and associated canopy PRI values.
120

121 ## 2. Methods

122 ### *2.1. Study Site and Field Data Collection*

123 During the summer of 2010, field campaigns were conducted on a corn crop (*Zea mays*
124 L.) in an experimental cornfield at the Optimizing Production Inputs for Economic and
125 Environmental Enhancement (OPE3) site (39.0304°N, 76.8458°W) maintained by the USDA
126 Beltsville Agricultural Research Center (BARC) in Beltsville, Maryland, U.S.A. Measurements
127 were acquired on three dates representing three different growth stages: an early vegetated
128 canopy when plants had nine fully expanded leaves (V9) and were ~1 m tall on 07/01; a fully

mature canopy having 13-15 fully expanded leaves at ~2 m tall in the early reproductive phase (VT) on 07/15; and an early senescent crop (~2 m tall) at the advanced reproductive development stage (R4) on 08/09. Canopy and leaf level measurements were taken along a 100-m north-south direction transect in the middle of the field to minimize disturbance and to maintain representativeness of the data. Hyperspectral reflectance (~1.5 nm Full Width Half Maximum; FWHM) was obtained for vegetation at both leaf and canopy levels and on bare soil using an USB4000 Miniature Fiber Optic Spectrometer (Ocean Optics Inc., Dunedin, FL, USA) with a bare fiber. *In situ* leaf reflectance observations were acquired directly adjacent to the adaxial leaf surfaces. The leaves were excised on the next day, and a Li-Cor 1800-12 integrating sphere (Li-Cor, Lincoln, NE, USA) paired with a spectroradiometer (FieldSpec, ASD Inc., Boulder, CO, USA) was utilized to determine transmittance from the leaf adaxial surfaces in the laboratory. At the canopy level, reflectance spectra were acquired at eight different relative azimuth angles (ψ, 0° to 315° relative to the sun, at 45° increments) coupled with three different view zenith angles (θ_v)-- 30°, 45°, 60° (obtained at 1.3, 0.75, 0.44 m above the canopy, respectively, to provide a consistent center of the field of view). Nadir ($\theta_v = 0°$; $\psi = 0°$) observations were acquired above the canopy at a height of approximately 1 m. This was accomplished by placing the fiber optics from a height-adjustable pole-mount, where a custom-made fixture was designed to position the instrument at a desired view zenith angle and relative azimuth angle. Soil background reflectance was taken on bare soil also approximately 1 m above the surface at nadir. Measurements were taken between local time 9 am to 4 pm, during which the solar zenith angle (θ_s) varied between 16.6° and 51.2° across the season. Crop LAI was also measured with a Li-Cor LAI-2000 plant canopy analyzer (Li-Cor, Lincoln, NE, USA). More detailed information regarding field data collections can be found in Cheng et al. (2010).

NOTE: The mention of trade names of commercial products in this article is solely for the purpose of providing specific information and does not imply recommendation or endorsement by the U.S. Department of Agriculture

2.2. Models and Simulation Methods

In this study, the canopy model ACRM (Kuusk, 1995a, b, 2001) was utilized to simulate PRI. This RT canopy model is equipped with an enhanced Markov chain bidirectional gap probability function that has been utilized in various studies using forward and inversion modes to validate and/or to estimate plants biochemical properties at leaf and/or canopy level (Cheng et al., 2010; Cheng et al., 2006; Fang et al., 2003; Houborg et al., 2009; Houborg et al., 2011). In our previous study, in which ACRM successfully simulated PRI for a young corn canopy, ACRM was set to run in its forward mode utilizing *in situ* leaf and soil background spectra to simulate canopy spectra at various viewing geometry (θ_v, ψ) configurations (Cheng et al., 2010). PRI was derived from the ACRM-simulated canopy reflectance spectra, and compared with the PRI derived from *in situ* canopy reflectance spectra. In this study, we followed the procedures presented in Cheng et al. (2010; 2011) and ran the model in two different modes: (i) with optical properties of sunlit leaves (only) in a single layer, or (ii) with both sunlit and shaded leaves in two layers, where the shaded layer laid below the sunlit layer. PRI was then derived from ACRM-simulated spectra and compared, as before, with PRI derived from *in situ* canopy reflectance spectra for validation. Values of other essential input parameters for the model are summarized in Table 1. These values came from either ancillary field measurements (e.g., LAI) or were decided based on previous studies (Cheng et al., 2010; Cheng et al., 2006; Fang et al., 2003; Houborg et al., 2009; Jacquemoud, 1993; Kuusk, 2001; Zarco-Tejada et al., 2003).

In Cheng et al. (2010; 2011), a sensitivity analysis was performed on several canopy structure parameters to investigate their effects on PRI simulations. The important influence of LAI on PRI simulations was reported. This study extends our progress and investigates how the vertical distribution and partitioning of LAI between the sunlit upper and the shaded lower canopy layers affect PRI simulations. In our earlier studies, when ACRM was set to run in the one layer mode, the LAI of the upper canopy was assumed to represent the total LAI, or 100%, such that the LAI fractions in upper/lower layers were 100% and 0% (i.e., 100/0). Likewise, when ACRM was set to run in the two layer mode, the LAI fractions of the upper and lower layers were assumed to equal half of the total LAI, (i.e., 50/50). In the current study, a sensitivity analysis was performed by changing the ratio of sunlit upper/shaded lower layer LAI values in 10% increments from 100/0 (fully sunlit) to 10/90 (mostly shaded).

3. RESULTS

3.1. In situ Leaf and Canopy Observations

Leaf-level PRI values derived from *in situ* leaf reflectance are summarized in Figure 1 as mean ± standard error (SE). PRI for sunlit leaves consistently exhibited lower values than shaded leaves on all three dates (ANOVA; n=60 for each day; 07/01, $p<0.0001$; 07/15, $p=0.0003$; 08/09, $p=0.001$). Average PRI values varied from -0.009 to +0.005 for sunlit leaves, and consistently exhibited negative values in the afternoons throughout the growing season. In contrast, mean PRI values for shaded leaves were always positive, varying from +0.002 to +0.022. PRI also showed higher mean values in the morning (AM) than in the afternoon (PM) on the two dates dominated by green foliage before senescence, especially for sunlit leaves (n=30, $p<0.001$ for both days). Among the three growth stages, PRI values were significantly higher for shaded

197 leaves (AM and PM) and sunlit leaves (AM) in the mature VT canopy (July 15) than on either
198 the early (V9) or later season (R4) growth stages (n=30, $p<0.0001$). At senescence, no clear
199 differences were observed between the morning and the afternoon (n=30, p=0.6 for sunlit;
200 p=0.48 for shaded leaves) but the pattern of higher PRI values for shaded vs. sunlit leaves was
201 maintained.

202 At the canopy level, *in situ* PRI values were plotted as mean ± SE against viewing
203 geometry (θ_v, ψ) for the three growth stages in Figure 2. The pattern obtained at leaf level (Fig.
204 1) for higher PRI at the VT stage (July 15) was maintained at the canopy level (-0.02 to +0.01)
205 when viewed over a range of view angles (θ_v , 0^o, 30^o, 45^o, and 60^o). Lower PRI values (-0.03 to
206 -0.01) occurred at both early (Fig.2, 07/01) and late stages (Fig.2, 08/09), which were similar in
207 their PRI responses at the smaller view zenith angles (0^o, n=48, p=0.44; 30°, n=128, p=0.16; 45^o,
208 n=128, p=0.06) as compared to mid-season VT stage. However, early and late growth stages
209 were differentiated by PRI values obtained at the extreme view, $\theta_v = 60^o$ (early > late, n= 128,
210 p=0.0011). PRI values at all azimuth positions increased as a function of θ_v. For example,
211 increases in the mean PRI at the coldspot ($\psi = 180^o$) for the VT canopy were: -0.003±0.005 at
212 30^o, 0.0±0.003 at 45^o, and +0.009±0.006 at 60^o. This contrasts with the negative PRI obtained at
213 nadir (-0.02±0.003), which would be interpreted as indicating greater physiological stress than
214 was determined at any other view. The general pattern exhibited for all measurement geometries
215 (8 ψ at 3 θ_v) was for PRI values to be lower when θ_v was close to 0° and highest when $\psi \approx 180°$
216 at any θ_v, highlighting the dependence on viewing geometries. Together, these results (Figs. 1,
217 2) demonstrate the influence of diurnal and directional effects on PRI values retrieved from a
218 cornfield.

3.2. ACRM-simulated PRI

Reflectance spectra were simulated as output from the ACRM. PRI values were calculated from those and compared with *in situ* PRI for validation purposes in Figure 3, where PRI values from both field measurements and simulations were plotted against θ_v and ψ (Fig. 3 a,c,e). ACRM-simulated PRI successfully captured the responses that *in situ* PRI exhibited to θ_v and ψ (Fig. 3 a,c,e), producing lower values when ψ was close to 0° and higher values when ψ was close to 180° at all θ_v on all three observation days. When the simulations were performed with sunlit leaves only, considerable underestimations as compared to *in situ* PRI values were observed (Fig. 3 a,c,e). The PRI underestimations were more pronounced on the young V9 crop (July 1) and the senescent R4 crop (August 9), but also occurred at smaller $\theta_v = 30^o$ for the mature VT crop. On the contrary, the differences between simulated and *in situ* values were much smaller, and in most cases not significant, when the simulation included both sunlit and shaded leaves (Figure 3a,c,e). Correlations between simulated vs. measured values are presented in Fig. 3b,d,f (panels on the right). The fully mature VT canopy (July 15, Fig. 3d) exhibited the highest correlation between *in situ* values and simulations under both scenarios: when both sunlit and shaded leaves were included ($r = 0.87$) and when only sunlit leaves were used ($r = 0.84$). The comparisons for the V9 canopy were also strong ($r = 0.78$, both sunlit and shaded leaves; $r = 0.80$, sunlit leaves only), although the sunlit (only) set is clearly offset from the 1:1 line. Results were weaker in the senescent R4 stage ($r = 0.65$, both sunlit and shaded leaves; $r = 0.52$, sunlit leaves only), with high variability-- especially for the sunlit dataset. Therefore, simulated PRI using both sunlit and shaded leaves (Fig. 3) yielded better correspondence (closer to the 1:1 line) on all three dates than simulations with only sunlit leaves. Statistics of comparisons between *in situ* and simulated PRI are summarized in Figure 4. For all three days,

when compared with *in situ* values, simulated PRI using both sunlit and shaded leaves (Fig. 4) generated significantly smaller root mean square error (RMSE) than simulations with sunlit leaves only (Fig. 4). Among the three days, simulated PRI showed the best agreement with *in situ* values at the VT stage, as evidenced by higher correlation coefficients ($r \geq 0.84$) and smaller RMSEs (≤ 0.0096) when the canopy was mature (Fig. 4).

The performance of ACRM-simulated PRI was further examined by calculating the difference from *in situ* values, which is summarized in Figure 5. The thick black line displayed in Fig. 5 indicates no (zero) difference between *in situ* and simulated values. Simulations performed using only sunlit leaves produced underestimations of field values, as shown by negative values (Fig. 5a). The largest underestimates (~0.03) were obtained at the two smaller view angles, nadir (0^o) and θ_v=30°. The only simulations with sunlit leaves alone that agreed with field measurements occurred for θ_v=60° in the forward scattering direction (ψ = 135° to 270°), for the fully green and mature mid-season VT canopy (Fig. 5a). When both sunlit and shaded leaves were used in simulations, the differences were much closer to zero (Fig. 5b), providing better agreements with *in situ* values under all observation and growth conditions. However, simulations done using both sunlit and shaded leaves for the VT canopy showed a small positive bias for part of the ψ range at all θ_v, whereas the differences appeared to scatter around zero at the other two growth stages (Fig. 5b).

3.3. Canopy Structure and PRI Simulations

The importance of taking optical properties of both sunlit and shaded leaves into account, as well as their relative proportions in the canopy, expressed as a canopy-level ratio, was further investigated using the mid-season VT canopy data. Figure 6 shows how the ACRM-simulated PRI values changed as a function of the sunlit/shaded canopy ratio and viewing geometry, for a

corn crop having LAI = 2.48. Columns with lighter shading indicate higher sunlit/shaded fractions. In the modeling scheme, a higher sunlit/shaded canopy ratio describes a canopy that is dominated by sunlit leaves, and therefore, optical properties of sunlit leaves influence the simulated canopy reflectances significantly more. On the contrary, a darker tone (Fig. 6) indicates lower sunlit/shaded canopy ratios were used to simulate situations where shaded leaves contributed more to the total canopy reflectance. Clearly, the PRI values obtained at any θ_v and ψ decrease as the sunlit/shaded canopy ratio favors more sunlit foliage (Fig. 6). A lower PRI value would indicate greater environmental stress, and reduced LUE. Therefore, for the same canopy LAI and growth stage, different inferences about LUE could be made based on the observed PRI, depending on viewing geometry and the inherent canopy structure profile. These results help explain why there have been so many confounding factors that influence the PRI of canopies that have been reported by various researchers.

These simulations were also directly compared with *in situ* PRI values (Figure 7), to reveal a linear shift away from the 1:1 line for the extreme cases, and displaying a general underestimation for the full sun (100/0) case, especially at lower PRI values, and a general overestimation for the mostly shaded (20/80) case. Statistics for the correlation coefficients and RMSEs are summarized in Figure 8, indicating the highest correlations paired with the lowest RMSE were associated with two groups in the mid-range (70/30, 60/40). The slope and offset of the regression lines (Figure 9), show a consistent decline for the slope (parameter "a") as the sunlit/shaded canopy ratio increasingly favored more shaded foliage, whereas the offset (parameter "b") increased. Since the best agreement between simulations and *in situ* observations was achieved for a 60/40 ratio, we can assume our field measurements were acquired at or near

287 the 60/40 sunlit/shaded canopy conditions. Thus, our original assumption of a 50/50 ratio was
288 not the optimal condition for the mature VT canopy in 2010.
289

290 ## 4. Discussion

291 The PRI was developed to track the reversible changes in the photoprotective xanthophyll
292 cycle induced by light intensity changes through a diurnal cycle, (Gamon et al., 1992; Peñuelas
293 et al., 1995). Subsequently, additional environmental stresses have been shown to influence the
294 pH of the chloroplast stroma, affecting the xanthophylls cycle and associated PRI values, such as
295 drought and cold temperatures (Demmig-Adams and Adams, 2000; Müller et al., 2001; Pfündel
296 and Bilger, 1994). Studies have also shown correlations between PRI and other
297 physiological/morphological changes, for instance, the carotenoids and chlorophyll ratio (Filella
298 et al., 2004; Sims and Gamon, 2002). In our previous study, we successfully demonstrated that in
299 *situ* leaf optical properties coupled with ACRM could simulate PRI for a young, homogeneous
300 corn canopy, still growing and in the vegetative growth stage. Here, we extended our study to
301 simulate PRI for a corn crop during three different growth stages during the 2010 growing
302 season.

303 ### *4.1. In situ PRI at Leaf and Canopy Level*

304 First of all, the results presented here confirm our previous studies showing that shaded
305 leaves captured in the coldspot of canopy directional reflectances have higher PRI values than
306 sunlit leaves (Cheng et al., 2010; Gamon et al., 1990; Middleton et al., 2009; Peñuelas et al.,
307 1995), and we extended those observations to examine the PRI responses through a growing
308 season in the same experimental cornfield location as the previous study. Higher PRI values in

shaded foliage and canopy sectors indicate that the intensity of xanthophyll-regulated photoprotection is lower than in sunlit leaves and canopy segments which are more likely to experience high light stress and exhibit lower PRI values. Furthermore, previous studies have shown correlations between leaf pigments (e.g. carotenoids/chlorophyll ratio) and PRI and the changes in PRI values could be related to leaf development and aging during the growing season (Garbulsky et al., 2011; Peñuelas et al., 2011).

Leaf level PRI for the "green" canopies (i.e., the V9 through VT growth stages) exhibited lower PRI values (i.e., greater stress) during afternoons after several hours of high irradiance exposure, than for mornings (Fig. 1). This pattern was also observed in our V10 dataset acquired in the same field in 2008 (Cheng et al., (2010), although the 2008 values were much higher, implying lower relative stress responses, which were very likely due to an abnormally wet spring that year. Higher PRI values were also obtained in shaded leaves vs. sunlit leaves in both morning and afternoon observations in the chlorophyll-dominated growth stages. For the senescent canopy, however, lower PRI values were found in shaded and sunlit leaves all day long. These lower mean PRI values for the senescent growth stage discriminated between shaded and sunlit (shaded > sunlit) but not AM vs. PM due to high variability (Fig. 1). Nevertheless, the importance of AM vs. PM observations in studying PRI vs. LUE or using PRI to determine LUE needs to be emphasized. The daily PRI averages followed the expected pattern: VT > V9 > R4, but the daily variation became large, as compared with either morning or afternoon observations. On the other hand, considerable error in estimating daily PRI values would be incurred if only sunlit foliage was considered on any of the dates examined, but especially for the mature, mid-season VT crop that had the largest sunlit vs. shaded PRI

difference. These findings should serve as a caution when utilizing daily average PRI values in model simulations of LUE at the ecosystem scale**.**

The canopy PRI observations showed substantial dependence on viewing geometry (Fig. 2), similar to results reported in our previous study (Cheng et al., 2010). PRI values were higher when the canopy was viewed at larger, oblique θ_v since more shaded foliage and less soil background contamination was captured. Secondly, PRI exhibited higher values when ψ was at the coldspot, close to 180° where the shaded dominated the field of view, and lower values when ψ was close to the hotspot at 0° (broadly including 45^o, 315°) where it was associated with the sunlit segment of the canopy (Fig. 2). This is a consistent pattern that has been observed in multiple years under different conditions for the cornfield and in forests (Hall et al., 2008; Hilker et al., 2008b; Huemmrich et al., 2009; Middleton et al., 2009). When utilizing spaceborne data, the observations are not always acquired at nadir (e.g., EO-1 Hyperion, Terra/Aqua MODIS). Therefore, this confounding effect needs to be addressed to retrieve meaningful information of plant physiological conditions from non-nadir as well as nadir PRI values. Previous studies conducted at a Douglas fir forest in British Columbia, Canada, also reported that PRI exhibited similar dependency to viewing geometry (Hall et al., 2008; Hilker et al., 2008b; Middleton et al., 2009), and are supported by a recent satellite study using off-nadir directional observations (Hall et al., 2011; Hilker et al., 2011).

PRI values at both leaf and canopy levels expressed less variance (e.g., smaller SE) in the young, homogeneous, unstressed V9 canopy (Figs. 1,2), with more variability accruing through the season as the crop aged, weathered, and experienced various unfavorable environmental conditions.

4.2. Simulation Performance and Differences in Previous Study

ACRM has been shown to successfully simulate canopy PRI values and their dependency on viewing geometry with the current 2010 data and with the previous 2008 data. ACRM was able to deliver believable simulations when both sunlit and shaded leaves were used (Fig. 3). However, when only sunlit leaves were included in the process, less agreement with field measurements was achieved and comparisons to *in situ* measurements produced higher RMSEs due to underestimation. The agreement with *in situ* PRI values was better when the corn crop was dominated by green foliage from the actively growing, early vegetative through the mature, reproductive growth stages. When the corn crop approached the senescent stage, ACRM simulation was satisfactory, but agreed with *in situ* values the least well among our datasets. The early senescent R4 crop, which had a lower leaf layer in the canopy comprised of brown (dead or low chlorophyll) leaves coupled with a mixed green/brown upper leaf canopy layer, exhibited relatively low PRI values (and high stress) in general, especially in the sunlit layer. The increasing complexity of the foliage distribution at this highly variable stage presents a challenge for simulations.

In our previous study, we showed that using sunlit and shaded leaves in the ACRM scheme can improve both the correlation and RMSE with *in situ* PRI values (Cheng et al., 2010). By considering the results from two field studies (2008, 2010), we can conclude that the most significant benefit of adding shaded leaves as the lower canopy layer in ACRM was to improve RMSE relative to field observations (see Fig.4 and Cheng et al., 2010). When ACRM was run in the one layer mode using only the optical properties of sunlit leaves, the simulated PRI showed satisfactory correlations with *in situ* values but had a significant offset, indicating an underestimate that could be incorrectly interpreted as a higher than actual physiological stress

response. This is an important issue since misinterpretation of PRI values will lead to significant errors in LUE and GPP estimates. This point was emphasized by calculating the difference between *in situ* and simulated PRI values for various viewing geometry and dates (Fig. 5) where simulations performed with only sunlit leaves obviously produced most of the underestimations as negative values (Fig. 5a). Small θ_v (nadir at 0^o and 30^o) had larger discrepancies than larger off-nadir views (45^o, 60^o), as compared with measurements. This is consistent with our previous study (Cheng et al., 2010), due in part to less soil background contamination at oblique angles. Among the three dates, discrepancies between field observations and "sunlit only" simulations were the smallest for the mature VT canopy (July 15, 2010), especially notable for $\theta_v = 60°$ (**X**), suggesting that at this oblique angle, sunlit leaves might dominate the field of view for a fully leafed out, green and erectophile canopy. We also note that the benefit of adding a shaded lower leaf layer for the VT canopy in the ACRM scheme, while advantageous, was less than on the other dates. This may be because the fully mature crop exhibited more sunlit leaves, greater canopy closure, and/or a well-developed vertical LAI profile. The latter factor has been shown to be temporally variant based on the growth stages of corn canopies (Ciganda et al., 2008).

4.3. Sunlit/Shaded Canopy Ratio

We tested various cases of variable sunlit/shaded canopy ratios, using our VT mature canopy dataset, for which the ACRM-simulated PRI values (for a given θ_v and ψ) were expected to increase when the sunlit/shaded ratio changed from 100/0 to 10/90. Those simulations (Fig. 6) duplicated those from the earlier study (Cheng et al. 2010): (1) the highest PRI values occurred at the coldspot ($\psi = 180^o$) and the lowest at the hotspot ($\psi = 0^o$); and (2) the PRI values were higher when θ_v increased from 30° to 60°. Therefore, in the ACRM simulations, changes to the

sunlit/shaded ratio affected the canopy PRI responses expected, but not the sensitivity to viewing geometry.

However, changes in the canopy structure could affect PRI values, causing underestimation or overestimation of "true" PRI values. When simulations were done with sunlit leaves only (100/0 in Fig. 7), most of the data points fell below the 1:1 line, underestimating, "true" field values. After adding optical properties of shaded leaves in the simulation, even for the 80/20 case, the data points moved closer to the 1:1 line and generated a ~50% improvement in RMSE (Fig. 7). On the other hand, when even more shaded leaves than sunlit leaves were included in the simulation (e.g., 40/60 and 20/80, Fig. 7), the simulated PRI moved up and over the 1:1 line, and generated higher RMSE due to overestimation. For this dataset, the simulated 60/40 sunlit/shaded canopy ratio appeared to have the best agreement with field measurements, and indicates that this was the likely field condition at that growth stage in 2010. Since these simulations used a homogeneous, fixed LAI (at 2.48), the sunlit dominated groups (e.g., 100/0 and 80/20) might indicate relatively more open canopies, made possible by longer stems and/or wider rows that put space between the leaves (since the number of leaves per plant is fixed). Likewise, the extreme case for a mostly shaded 20/80 canopy has a more compact, closely spaced leaf arrangement along a short stem, and/or a closed canopy in narrower rows.

Results summarized in Tab. 2 also confirm the importance of adding shaded leaves into the simulation scheme, since even when using a 80/20 ratio as the input, significant improvement in RMSE (~30% to 50%) can be achieved. For the mature VT canopy, even though the 60/40 ratio appeared to be optimal by generating the best agreement of the sunlit/shaded ratio to *in situ* measurements ($r = 0.87$; RMSE = 0.0045), the performance using 50/50 was still quite close ($r = 0.87$; RMSE = 0.0048). Furthermore, after finding that the 50/50 sunlit/shaded ratio was not the

optimal value to generate the best simulations for the mature VT canopy, we investigated the issue for the other two dates in 2010 and one V10 dataset acquired on August 1, 2008 (Tab. 2). For all three of these other datasets, the 50/50 sunlit/shaded ratio did appear to be optimal for simulating canopy PRI, based on better statistical performances (higher correlation coefficients and lower RMSEs). Therefore, while additional canopy structure information might improve PRI values interpretation and simulation in a cornfield using ACRM, the 50/50 sunlit/shaded ratio will generate more than satisfactory results for most of the cases.

These results indicate that the sunlit/shaded ratio, a structure-based parameter, may change within a growing season. Therefore, this sensitivity analysis highlights the importance of canopy structure in simulating and understanding PRI. The implication is that since different vegetation types have different canopy structures (e.g., forests vs. crops vs. shrubs), our on-going and future research will apply this modeling scheme to different vegetation functional types. More importantly, most approaches have assumed that the sunlit upper canopy is the major contributor and regulator of GPP/NPP, and that either the shaded component can be largely ignored or the whole system is assumed to operate in one mode (e.g., sunlit) for total canopy foliage amount defined by LAI. Our results suggest that only taking sunlit leaves into account would lead to underestimation of canopy PRI values, implying greater than actual stress levels and leading to underestimates of LUE and GPP. Previous studies have also recognized the importance of separating sunlit and shaded leaves for modeling photosynthetic activities from leaf to canopy level (Chen et al., 1999; De Pury and Farquhar, 1997; Wang and Leuning, 1998) mostly due to the nonlinear response of leaf carbon assimilation to light intensity. Adding spectral information about the shaded canopy foliage is critical for improving our understanding about canopy physiological processes, and our ability to simulate PRI and related parameters.

444 Improvement in understanding PRI information will potentially reduce uncertainties in LUE
445 estimates using remote sensing observations and advance carbon uptake monitoring capabilities.
446

447 ## 5. SUMMARY

448 In this study, we examined the capability of coupling *in situ* leaf optical properties and
449 ACRM to simulate canopy level PRI at various growth stages of a corn crop. ACRM-simulated
450 canopy PRI values were closer to field measurements when both sunlit and shaded leaves were
451 utilized in the scheme. The performance of the model was greatly improved when the crop was
452 dominated by green foliage during the vegetative and mature reproductive stages. The least
453 satisfactory results were found when the corn crop reached the senescent stage. The significance
454 of taking both sunlit and shaded leaf segments into account for canopy PRI studies was
455 presented. We further examined how variable sunlit/shaded canopy ratios affected the modeled
456 results. Simulated canopy PRI values increased as the contribution from the shaded fraction
457 increased (i.e., the sunlit/shaded ratio decreased). The analysis suggested that canopy structure
458 information might be needed to improve simulations or to interpret PRI. These findings also
459 imply that canopy PRI investigations and simulations should be investigated for more plant
460 functional types.
461

462 ## ACKNOWLEDGEMENTS

463 This study was supported by a NASA ROSES project (PI, E.M. Middleton) funded through the
464 Carbon Cycle Science Program (Diane Wickland, manager). The authors gratefully acknowledge
465 A. Kuusk for sharing computer code for the canopy reflectance model, and K.F. Huemmrich
466 (UMBC), P.K.E. Campbell (UMBC), A. Russ (USDA-ARS Hydrology and Remote Sensing

Lab) and D. Lagomasino (FIU) for assisting field campaign and their valuable comments. The authors thank the anonymous reviewers for their very valuable suggestions and criticism.

REFERENCES

Anderson, M.C., Norman, J.M., Meyers, T.P., & Diak, G.R. (2000). An analytical model for estimating canopy transpiration and carbon assimilation fluxes based on canopy light-use efficiency. *Agricultural and Forest Meteorology, 101* (4), 265-289.

Barton, C.V.M., & North, P.R.J. (2001). Remote sensing of canopy light use efficiency using the photochemical reflectance index: Model and sensitivity analysis. *Remote Sensing of Environment, 78* (3), 264-273.

Chen, J.M., Liu, J., Cihlar, J., & Goulden, M.L. (1999). Daily canopy photosynthesis model through temporal and spatial scaling for remote sensing applications. *Ecological Modelling, 124* (2-3), 99-119.

Cheng, Y.-B., Middleton, E.M., Hilker, T., Coops, N.C., Krishnan, P., & Black, T.A. (2009). Dynamics of spectral bio-indicators and their correlations with light use efficiency using directional observations at a Douglas-fir forest. *Measurement Science and Technology, 20* (9), 095107.

Cheng, Y.-B., Middleton, E.M., Huemmrich, K.F., Zhang, Q., Campbell, P.K.E., Corp, L.A., Russ, A.L., & Kustas, W.P. (2010). Utilizing *in situ* directional hyperspectral measurements to validate bio-indicator simulations for a corn crop canopy. *Ecological Informatics, 5* (5), 330-338.

Cheng, Y.-B., Middleton, E.M., Huemmrich, K.F., Zhang, Q., Corp, L., Campbell, P., & Kustas, W. (2011). Spectral bio-indicator simulations for tracking photosynthetic activities in a corn field. *In, SPIE Optics and Photonics 2011*. San Diego, CA, USA. 21-25 August 2011.

Cheng, Y.-B., Zarco-Tejada, P.J., Riano, D., Rueda, C.A., & Ustin, S.L. (2006). Estimating vegetation water content with hyperspectral data for different canopy scenarios: Relationships between AVIRIS and MODIS indexes. *Remote Sensing of Environment, 105* (4), 354-366.

Ciganda, V., Gitelson, A., & Schepers, J. (2008). Vertical profile and temporal variation of chlorophyll in maize canopy: Quantitative "crop vigor" indicator by means of reflectance-based techniques. *Agronomy Journal, 100* (5), 1409-1417.

Coops, N.C., Hilker, T., Hall, F.G., Nichol, C.J., & Drolet, G.G. (2010). Estimation of Light-use Efficiency of Terrestrial Ecosystems from Space: A Status Report. *Bioscience, 60* (10), 788-797.

De Pury, D.G.G., & Farquhar, G.D. (1997). Simple scaling of photosynthesis from leaves to canopies without the errors of big-leaf models. *Plant, Cell & Environment, 20* (5), 537-557.

Demmig-Adams, B., & Adams III, W.W. (1996). The role of xanthophyll cycle carotenoids in the protection of photosynthesis. *Trends in Plant Science, 1* (1), 21-26.

Demmig-Adams, B., & Adams, W.W. (2000). Photosynthesis: Harvesting sunlight safely. *Nature, 403* (6768), 371-374.

Drolet, G.G., Huemmrich, K.F., Hall, F.G., Middleton, E.M., Black, T.A., Barr, A.G., & Margolis, H.A. (2005). A MODIS-derived photochemical reflectance index to detect inter-annual variations in the photosynthetic light-use efficiency of a boreal deciduous forest. *Remote Sensing of Environment, 98* (2-3), 212-224.

Fang, H., Liang, S., & Kuusk, A. (2003). Retrieving leaf area index using a genetic algorithm with a canopy radiative transfer model. *Remote Sensing of Environment, 85* (3), 257-270.

Filella, I., Amaro, T., Araus, J.L., & Peñuelas, J. (1996). Relationship between photosynthetic radiation-use efficiency of barley canopies and the photochemical reflectance index (PRI). *Physiologia Plantarum, 96* (2), 211-216.

Filella, I., Peñuelas, J., Llorens, L., & Estiarte, M. (2004). Reflectance assessment of seasonal and annual changes in biomass and CO2 uptake of a Mediterranean shrubland submitted to experimental warming and drought. *Remote Sensing of Environment, 90* (3), 308-318.

Gamon, J., Field, C., Fredeen, A., & Thayer, S. (2001). Assessing photosynthetic downregulation in sunflower stands with an optically-based model. *Photosynthesis Research, 67* (1), 113-125.

Gamon, J.A., Field, C.B., Bilger, W., Björkman, O., Fredeen, A.L., & Peñuelas, J. (1990). Remote sensing of the xanthophyll cycle and chlorophyll fluorescence in sunflower leaves and canopies. *Oecologia, 85* (1), 1-7.

Gamon, J.A., Field, C.B., Roberts, D.A., Ustin, S.L., & Valentini, R. (1993). Functional patterns in an annual grassland during an AVIRIS overflight. *Remote Sensing of Environment, 44* (2/3), 239-253.

Gamon, J.A., Penuelas, J., & Field, C.B. (1992). A narrow-waveband spectral index that tracks diurnal changes in photosynthetic efficiency. *Remote Sensing of Environment, 41* (1), 35-44.

Gamon, J.A., Serrano, L., & Surfus, J.S. (1997). The photochemical reflectance index: an optical indicator of photosynthetic radiation use efficiency across species, functional types, and nutrient levels. *Oecologia, 112* (4), 492-501.

Garbulsky, M.F., Peñuelas, J., Gamon, J., Inoue, Y., & Filella, I. (2011). The photochemical reflectance index (PRI) and the remote sensing of leaf, canopy and ecosystem radiation use efficiencies: A review and meta-analysis. *Remote Sensing of Environment, 115* (2), 281-297.

Garbulsky, M.F., PeÑUelas, J., Papale, D., & Filella, I. (2008). Remote estimation of carbon dioxide uptake by a Mediterranean forest. *Global Change Biology, 14* (12), 2860-2867.

Gower, S.T., Kucharik, C.J., & Norman, J.M. (1999). Direct and indirect estimation of leaf area index, fAPAR, and net primary production of terrestrial ecosystems. *Remote Sensing of Environment, 70* (1), 29-51.

Hall, F.G., Hilker, T., & Coops, N.C. (2011). PHOTOSYNSAT, photosynthesis from space: Theoretical foundations of a satellite concept and validation from tower and spaceborne data. *Remote Sensing of Environment, 115* (8), 1918-1925.

Hall, F.G., Hilker, T., & Coops, N.C. (2012). Data assimilation of photosynthetic light-use efficiency using multi-angular satellite data: I. Model formulation. *Remote Sensing of Environment, 121* (0), 301-308.

Hall, F.G., Hilker, T., Coops, N.C., Lyapustin, A., Huemmrich, K.F., Middleton, E., Margolis, H., Drolet, G., & Black, T.A. (2008). Multi-angle remote sensing of forest light use efficiency by observing PRI variation with canopy shadow fraction. *Remote Sensing of Environment, 112* (7), 3201-3211.

Heinsch, F.A., Reeves, M.C., Votava, P., Kang, S., Milesi, C., Zhao, M., Glassy, J., Jolly, W.M., Loehman, R., Bowker, C.F., Kimball, J.S., Nemani, R.R., & Running, S.W. (2003). User's Guide: GPP and NPP (MOD17A2/A3) Products, NASA MODIS Land Algorithm. *University of Motana, Missoula, MT,* .

555 Heinsch, F.A., Zhao, M., Running, S.W., Kimball, J.S., Nemani, R.R., Davis, K.J., Bolstad, P.V.,
556 Cook, B.D., Desai, A.R., Ricciuto, D.M., Law, B.E., Oechel, W.C., Kwon, H., Luo, H.,
557 Wofsy, S.C., Dunn, A.L., Munger, J.W., Baldocchi, D.D., Xu, L., Hollinger, D.Y.,
558 Richardson, A.D., Stoy, P.C., Siqueira, M.B.S., Monson, R.K., Burns, S.P., & Flanagan, L.B.
559 (2006). Evaluation of remote sensing based terrestrial productivity from MODIS using
560 regional tower eddy flux network observations. *IEEE Transactions on Geoscience and*
561 *Remote Sensing, 44* (7), 1908-1925.
562 Hernández-Clemente, R., Navarro-Cerrillo, R.M., Suárez, L., Morales, F., & Zarco-Tejada, P.J.
563 (2011). Assessing structural effects on PRI for stress detection in conifer forests. *Remote*
564 *Sensing of Environment, 115* (9), 2360-2375.
565 Hilker, T., Coops, N.C., Hall, F.G., Black, T.A., Chen, B., Krishnan, P., Wulder, M.A., Sellers,
566 P.J., Middleton, E.M., & Huemmrich, K.F. (2008a). A modeling approach for upscaling
567 gross ecosystem production to the landscape scale using remote sensing data. *Journal of*
568 *Geophysical Research - Biogeosciences, 113* G03006.
569 Hilker, T., Coops, N.C., Hall, F.G., Black, T.A., Wulder, M.A., Nesic, Z., & Krishnan, P.
570 (2008b). Separating physiologically and directionally induced changes in PRI using BRDF
571 models. *Remote Sensing of Environment, 112* (6), 2777-2788.
572 Hilker, T., Coops, N.C., Hall, F.G., Nichol, C.J., Lyapustin, A., Black, T.A., Wulder, M.A.,
573 Leuning, R., Barr, A., Hollinger, D.Y., Munger, B., & Tucker, C.J. (2011). Inferring
574 terrestrial photosynthetic light use efficiency of temperate ecosystems from space. *J.*
575 *Geophys. Res., 116* (G3), G03014.
576 Hilker, T., Hall, F.G., Tucker, C.J., Coops, N.C., Black, T.A., Nichol, C.J., Sellers, P.J., Barr, A.,
577 Hollinger, D.Y., & Munger, J.W. (2012). Data assimilation of photosynthetic light-use

578 efficiency using multi-angular satellite data: II Model implementation and validation. *Remote*
579 *Sensing of Environment, 121* (0), 287-300.
580 Houborg, R., Anderson, M., & Daughtry, C. (2009). Utility of an image-based canopy
581 reflectance modeling tool for remote estimation of LAI and leaf chlorophyll content at the
582 field scale. *Remote Sensing of Environment, 113* (1), 259-274.
583 Houborg, R., Anderson, M.C., Daughtry, C.S.T., Kustas, W.P., & Rodell, M. (2011). Using leaf
584 chlorophyll to parameterize light-use-efficiency within a thermal-based carbon, water and
585 energy exchange model. *Remote Sensing of Environment, 115* (7), 1694-1705.
586 Huemmrich, K.F., Middleton, E.M., Landis, D., Black, T.A., B., A., McCaughey, J.H., & Hall,
587 F.G. (2009). Remote sensing of light use efficiency. *In, Proceedings of the 30th Canadian*
588 *Symposium on Remote Sensing.* Lethbridge, Alberta, Canada. June 22-25, 2009.
589 Inoue, Y., Peñuelas, J., Miyata, A., & Mano, M. (2008). Normalized difference spectral indices
590 for estimating photosynthetic efficiency and capacity at a canopy scale derived from
591 hyperspectral and CO2 flux measurements in rice. *Remote Sensing of Environment, 112* (1),
592 156-172.
593 Jacquemoud, S. (1993). Inversion of the PROSPECT + SAIL canopy reflectance model from
594 AVIRIS equivalent spectra: Theoretical study. *Remote Sensing of Environment, 44* (2/3),
595 281-292.
596 Jacquemoud, S., Ustin, S.L., Verdebout, J., Schmuck, G., Andreoli, G., & Hosgood, B. (1996).
597 Estimating leaf biochemistry using the PROSPECT leaf optical properties model. *Remote*
598 *Sensing of Environment, 56* (3), 194-202.
599 King, D.A., Turner, D.P., & Ritts, W.D. (2011). Parameterization of a diagnostic carbon cycle
600 model for continental scale application. *Remote Sensing of Environment, 115* (7), 1653-1664.

601 Kuusk, A. (1995a). A fast, invertible canopy reflectance model. *Remote Sensing of Environment,*
602 *51* (3), 342-350.
603 Kuusk, A. (1995b). A Markov chain model of canopy reflectance. *Agricultural and Forest*
604 *Meteorology, 76* (3-4), 221-236.
605 Kuusk, A. (2001). A two-layer canopy reflectance model. *Journal of Quantitative Spectroscopy*
606 *and Radiative Transfer, 71* (1), 1-9.
607 Law, B.E., & Waring, R.H. (1994). Combining remote sensing and climatic data to estimate net
608 primary production across Oregon. *Ecological Applicaitons, 4* (4), 717-728.
609 Lin, J.C., Pejam, M.R., Chan, E., Wofsy, S.C., Gottlieb, E.W., Margolis, H.A., & McCaughey,
610 J.H. (2011). Attributing uncertainites in simulated biospheric carbon fluxes to different error
611 sources. *Global Biogeochemical Cycles (in press)*
612 Mahadevan, P., Wofsy, S.C., Matross, D.M., Xiao, X., Dunn, A.L., Lin, J.C., Gerbig, C.,
613 Munger, J.W., Chow, V.Y., & Gottlieb, E.W. (2008). A satellite-based biosphere
614 parameterization for net ecosystem CO2 exchange: Vegetation Photosynthesis and
615 Respiration Model (VPRM). *Global Biogeochem. Cycles, 22* (2), GB2005.
616 Middleton, E.M., Cheng, Y.-B., Hilker, T., Black, T.A., Krishnan, P., Coops, N.C., &
617 Huemmrich, K.F. (2009). Linking foliage spectral responses to canopy level ecosystem
618 photosynthetic light use efficiency at a Douglas-fir forest in Canada. *Canadian Journal of*
619 *Remote Sensing, 35* (2), 166-188.
620 Middleton, E.M., Huemmrich, K.F., Cheng, Y.-B., & Margolis, H.A. (2011). Spectral
621 bioindicators of photosynthetic efficiency and vegetation stress. In P.S. Thenkabail, J.G.
622 Lyon & A. Huete (Eds.), *Hyperspectral Remote Sensing of Vegetation* (pp. 265-288): CRC
623 Press.

624 Monteith, J.L. (1972). Solar-radiation and productivity in tropical ecosystems. *journal of Applied*
625 *Ecology, 9* (3), 747-766.
626 Monteith, J.L. (1977). Climate and the efficiency of crop production in Britain. *Philosophical*
627 *Transaction of the Royal Society of London. Series B: Biological Sciences, 281* (980), 277-
628 294.
629 Müller, P., Li, X.-P., & Niyogi, K.K. (2001). Non-photochemical quenching. A response to
630 excess light energy. *Plant Physiology, 125* (4), 1558-1566.
631 Nichol, C.J., & Grace, J. (2010). Determination of leaf pigment content in Calluna vulgaris
632 shoots from spectral reflectance. *International Journal of Remote Sensing, 31* (20), 5409-
633 5422.
634 Nichol, C.J., Lloyd, J., Shibistova, O., Arneth, A., Röser, C., Knohl, A., Matsubara, S., & Grace,
635 J. (2002). Remote sensing of photosynthetic-light-use efficiency of a Siberian boreal forest.
636 *Tellus, 54B* (5), 677-687.
637 Peñuelas, J., Filella, I., & Gamon, J.A. (1995). Assessment of photosynthetic radiation-use
638 efficiency with spectral reflectance. *New Phytologist, 131* (3), 291-296.
639 Peñuelas, J., Garbulsky, M.F., & Filella, I. (2011). Photochemical reflectance index (PRI) and
640 remote sensing of plant CO2 uptake. *New Phytologist, 191* (3), 596-599.
641 Peñuelas, J., & Inoue, Y. (2000). Reflectance assessment of canopy CO2 uptake. *International*
642 *Journal of Remote Sensing, 21* (17), 3353-3356.
643 Peñuelas, J., Llusia, J., Pinol, J., & Filella, I. (1997). Photochemical reflectance index and leaf
644 photosynthetic radiation-use-effeciency assessment in Mediterranean trees. *International*
645 *Journal of Remote Sensing, 18* (13), 2863-2868.

Pfündel, E.E., & Bilger, W. (1994). Regulation and possible function of the violaxanthin cycle. *Photosynthesis Research, 42* (2), 89-109.

Prince, S.D., & Goward, S.N. (1995). Global primary production: A remote sensing approach. *Journal of Biogeography, 22* (4-5), 815-835.

Sims, D.A., & Gamon, J.A. (2002). Relationships between leaf pigment content and spectral reflectance across a wide range of species, leaf structures and developmental stages. *Remote Sensing of Environment, 81* (2-3), 337-354.

Sims, D.A., Luo, H., Hastings, S., Oechel, W.C., Rahman, A.F., & Gamon, J.A. (2006). Parallel adjustments in vegetation greenness and ecosystem CO2 exchange in response to drought in a Southern California chaparral ecosystem. *Remote Sensing of Environment, 103* (3), 289-303.

Stylinski, Gamon, & Oechel (2002). Seasonal patterns of reflectance indices, carotenoid pigments and photosynthesis of evergreen chaparral species. *Oecologia, 131* (3), 366-374.

Suárez, L., Zarco-Tejada, P.J., Berni, J.A.J., González-Dugo, V., & Fereres, E. (2009). Modelling PRI for water stress detection using radiative transfer models. *Remote Sensing of Environment, 113* (4), 730-744.

Verhoef, W. (1984). Light scattering by leaf layers with application to canopy reflectance modeling: The SAIL model. *Remote Sensing of Environment, 16* (2), 125-141.

Wang, Y.P., & Leuning, R. (1998). A two-leaf model for canopy conductance, photosynthesis and partitioning of available energy I:: Model description and comparison with a multi-layered model. *Agricultural and Forest Meteorology, 91* (1-2), 89-111.

667 Xiao, X., Zhang, Q., Braswell, B., Urbanski, S., Boles, S., Wofsy, S., Moore III, B., & Ojima, D.
668 (2004). Modeling gross primary production of temperate deciduous broadleaf forest using
669 satellite images and climate data. *Remote Sensing of Environment, 91* (2), 256-270.
670 Zarco-Tejada, P.J., Rueda, C.A., & Ustin, S.L. (2003). Water content estimation in vegetation
671 with MODIS reflectance data and model inversion methods. *Remote Sensing of Environment,*
672 *85* (1), 109-124.
673 Zhang, Q., Middleton, E.M., Gao, B.-C., & Cheng, Y.-B. (2011). Using EO-1 Hyperion to
674 simulate HyspIRI products for a coniferous forest: the fraction of PAR absorbed by
675 chlorophyll (fAPARchl) and leaf water content (LWC). *Geoscience and Remote Sensing,*
676 *IEEE Transactions on, 50*(5), 1844-1852.
677
678

FIGURE CAPTIONS

Figure 1. PRI values derived from *in situ* leaf reflectance for the sunlit (□) and shaded (■) leaves used as input data in the simulations and daily average (■) on three field days in 2010. Values are shown as mean ± SE.

Figure 2. *In situ* canopy PRI values from field measurements are shown for nadir (θ_v=0°; ψ=0°) and for three additional view zenith angles (θ_v=30°,45°,60°) which were coupled with eight relative azimuth angles (ψ=0° to 315° with 45° increment) on July 1st (■), July 15th (■), and August 9th (□) in 2010. Values are shown as mean ± SE. The mature canopy was clearly differentiated from early and late canopies, with higher PRI values at any θ_v. Early and late growth stages were similar at θ_v = 30^o and 45^o, but were differentiated at θ_v = 60^o. These results were used as validation data for simulations.

Figure 3. Comparisons and regressions between simulated and *in situ* PRI values on three days during the 2010 growing season: (a)(b) July 1; (c)(d) July 15; and (e)(f) August 9. Simulations were performed using either sunlit leaves only (◇) or both sunlit and shaded leaves (▲). Values are shown as mean ± SE. in (a)(c)(e). In general, simulations agreed with field observations when both sunlit and shaded foliage were included.

Figure 4. Summary chart of statistics representing all data collected on the three 2010 field dates, for simulations using either sunlit canopy only or both sunlit and shaded canopy sectors: (a) correlation coefficient (r) and (b) root mean square error (RMSE) relating *in situ* and simulated PRI values.

Figure 5. Differences between values for *in situ* versus simulated PRI plotted against viewing geometry (θ_v and ψ) for the three growth stages in 2010. The black dashed line indicates zero

difference between *in situ* and simulated values. Discrepancies indicate the error incurred in simulations.

Figure 6. Changes in PRI values when 2-layer simulations were performed with various sunlit/shaded canopy ratios, where the upper layer is sunlit and the lower layer is shaded. Simulations were done using parameters from the mature and green VT canopy, LAI = 2.48 on July 15, 2010. Six sunlit/shaded ratio cases were investigated, as shown in the label, represented by increasingly darker grey tone as more shaded leaves are included. The nadir case is included in the top panel.

Figure 7. Correlations between *in situ* PRI measurements and PRI values simulated using various sunlit/shaded canopy ratios, for the mature VT canopy on July 15, 2010. LAI = 2.48.

Figure 8. Statistics for the correlation coefficient (r) and root mean square error (RMSE), relating *in situ* PRI measurements and simulated PRI values across various sunlit/shaded canopy ratios. Based on the VT canopy (July 15, 2010; LAI = 2.48).

Figure 9. Parameters of the regression line (y=ax+b) relating *in situ* and simulated PRI values, using various sunlit/shaded canopy ratios. Parameter "a" is the slope while "b" is the offset of the regression line. Based on the VT canopy (July 15, 2010; LAI = 2.48).

TABLE CAPTIONS

Table 1. Value or range of parameters used as input to ACRM in this study.

Table 2. Correlation coefficients (r) and root mean square errors (RMSE) relating *in situ* PRI measurements and ACRM-simulated PRI values using various sunlit/shaded canopy ratios are presented for three additional days: an early 2008 growth stage and two 2010 growth stages.

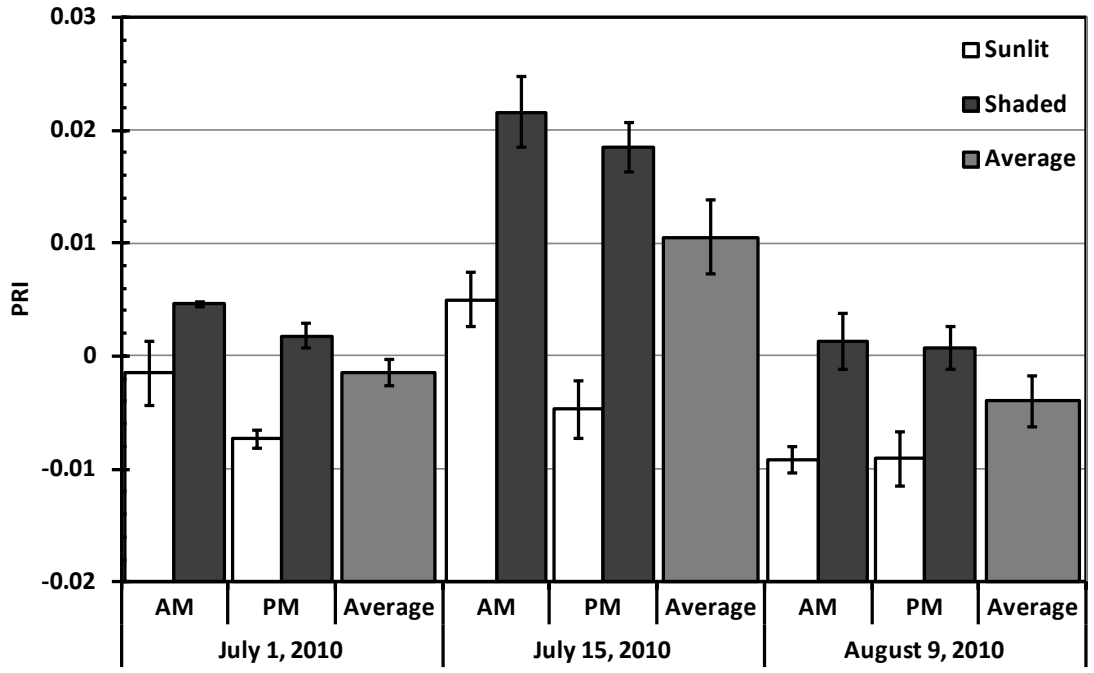

724
725 **Figure 1.** PRI values derived from *in situ* leaf reflectance for the sunlit (□) and shaded (■)
726 leaves used as input data in the simulations and daily average (■) on three field days in 2010.
727 Values are shown as mean ± SE.

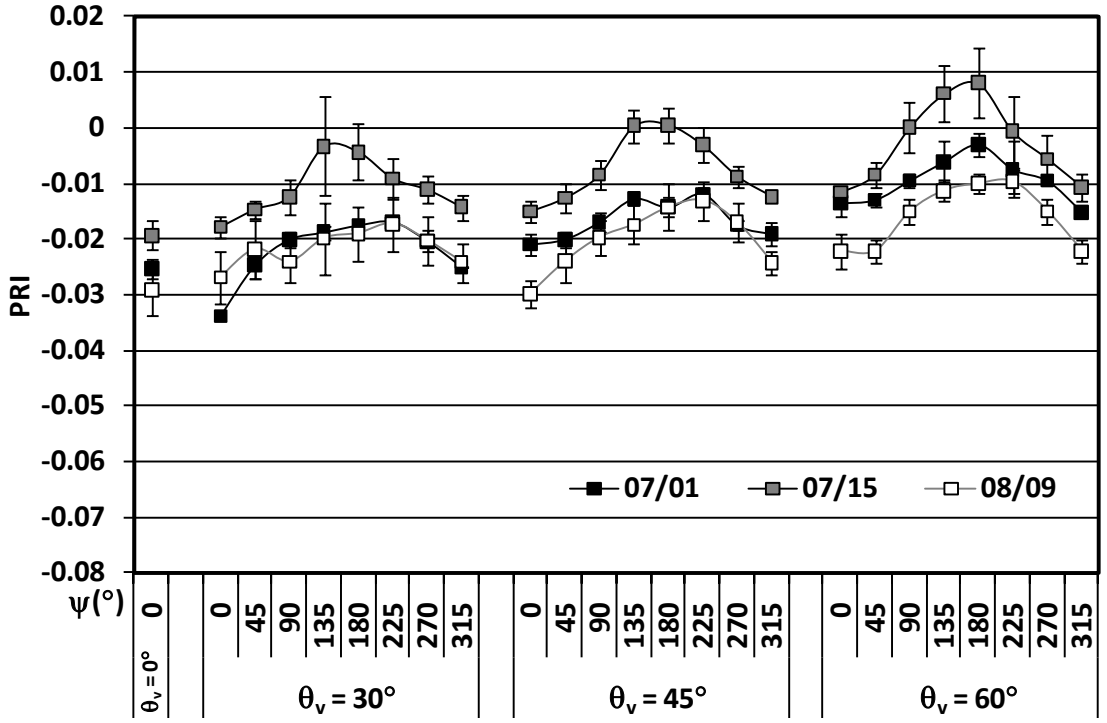

Figure 2. *In situ* canopy PRI values from field measurements are shown for nadir (θ_v=0°; ψ=0°) and for three additional view zenith angles (θ_v=30°,45°,60°) which were coupled with eight relative azimuth angles (ψ=0° to 315° with 45° increment) on July 1st (■), July 15th (■), and August 9th (□) in 2010. Values are shown as mean ± SE. The mature canopy was clearly differentiated from early and late canopies, with higher PRI values at any θ_v. Early and late growth stages were similar at θ_v = 30° and 45°, but were differentiated at θ_v = 60°. These results were used as validation data for simulations.

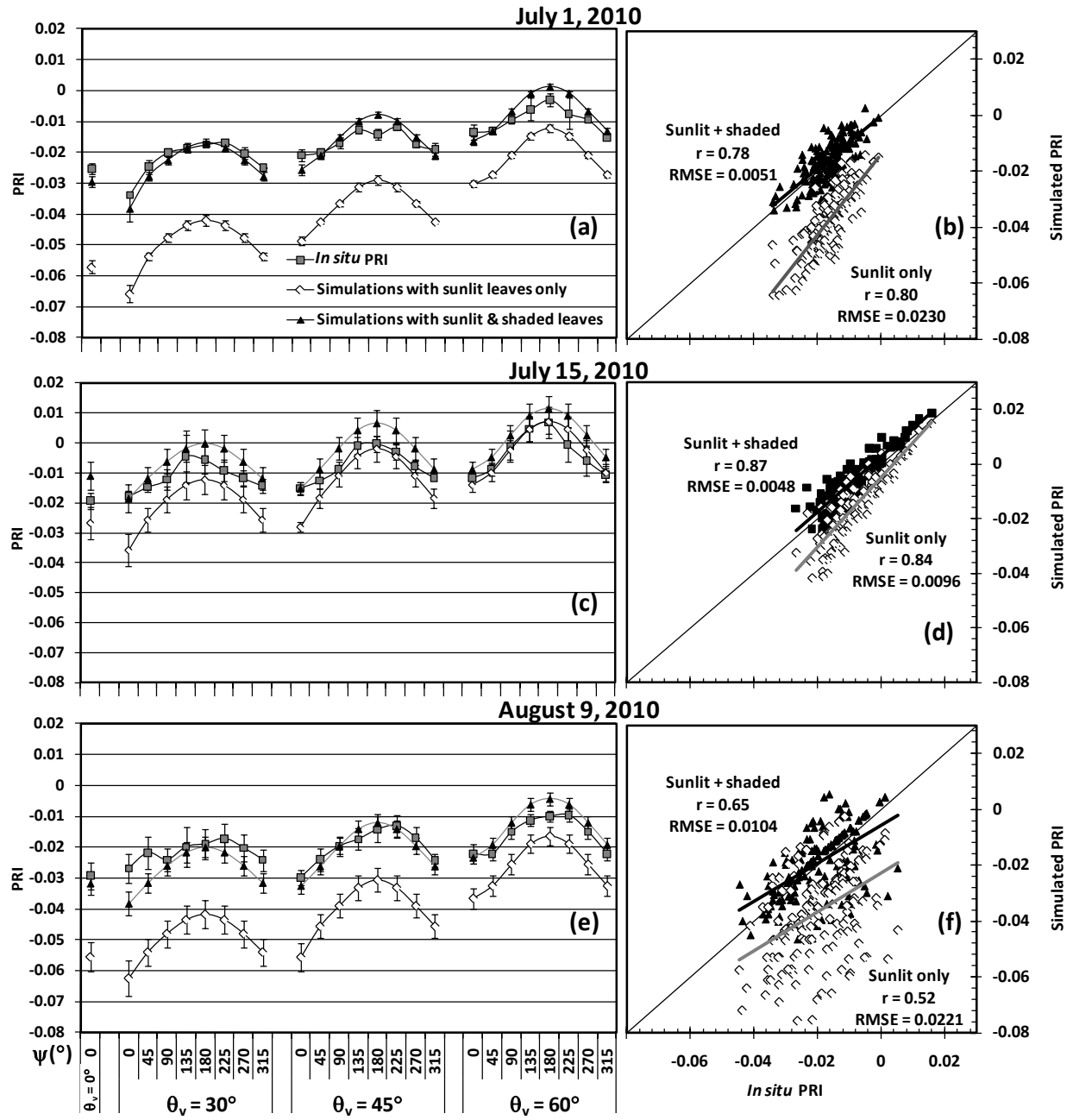

Figure 3. Comparisons and regressions between simulated and *in situ* PRI values on three days during the 2010 growing season: (a)(b) July 1; (c)(d) July 15; and (e)(f) August 9. Simulations were performed using either sunlit leaves only (◇) or both sunlit and shaded leaves (▲). Values are shown as mean ± SE. in (a)(c)(e). In general, simulations agreed with field observations when both sunlit and shaded foliage were included.

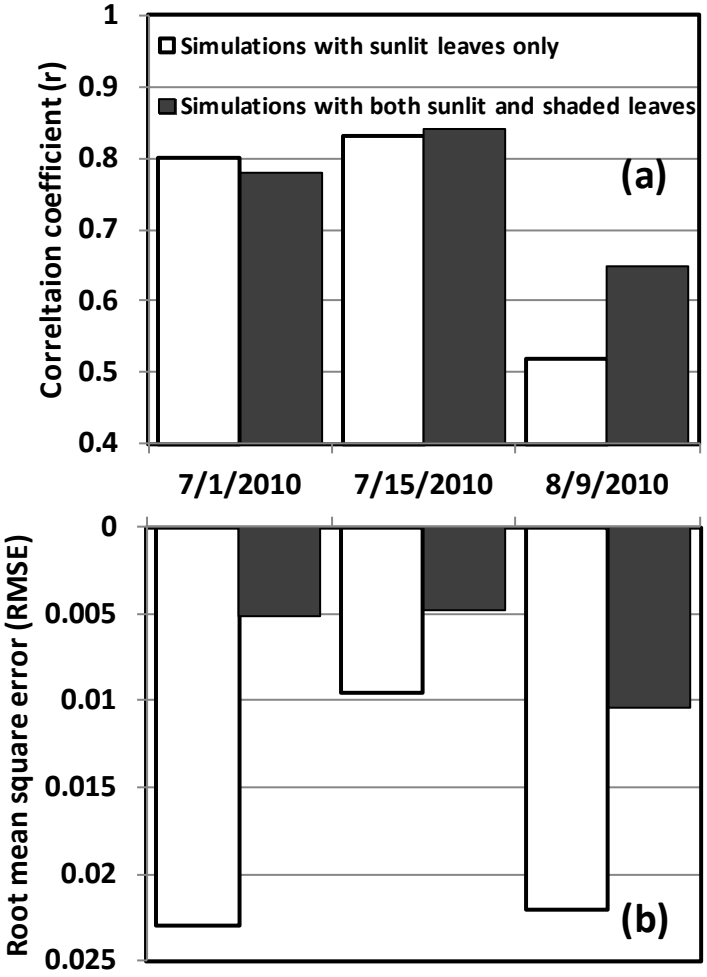

744
745 **Figure 4.** Summary chart of statistics representing all data collected on the three 2010 field
746 dates, for simulations using either sunlit canopy only or both sunlit and shaded canopy sectors:
747 (a) correlation coefficient (r) and (b) root mean square error (RMSE) relating *in situ* and
748 simulated PRI values.

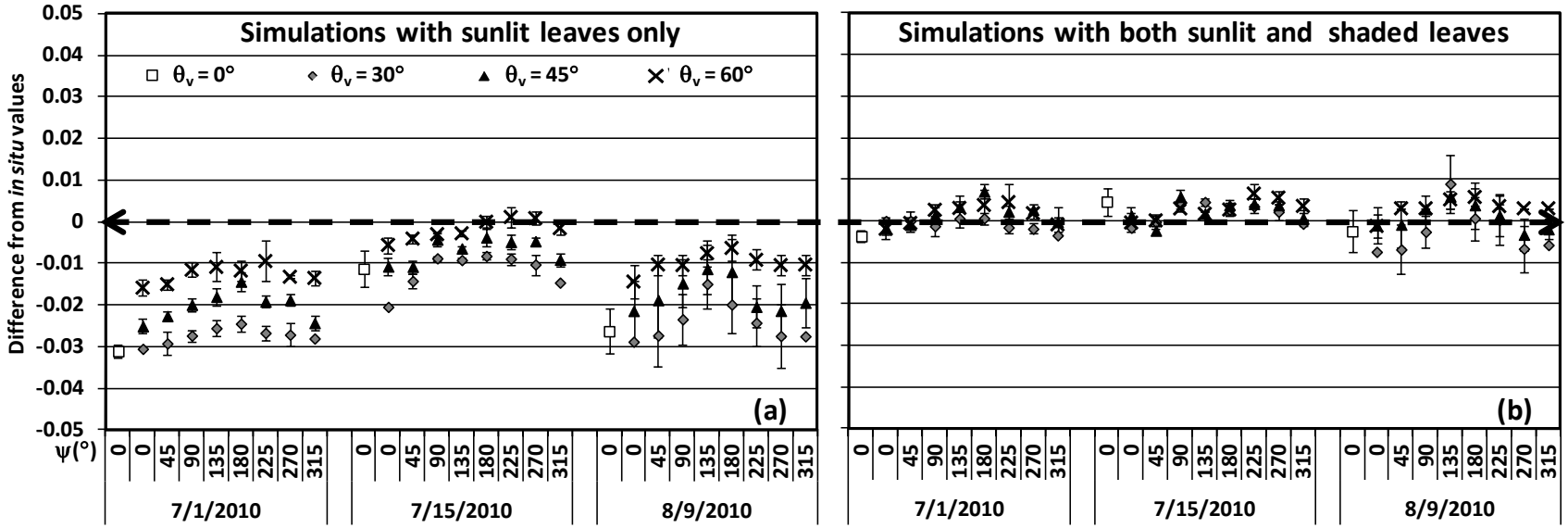

Figure 5. Differences between values for *in situ* versus simulated PRI plotted against viewing geometry (θ_v and ψ) for the three growth stages in 2010. The black dashed line indicates zero difference between *in situ* and simulated values. Discrepancies indicate the error incurred in simulations.

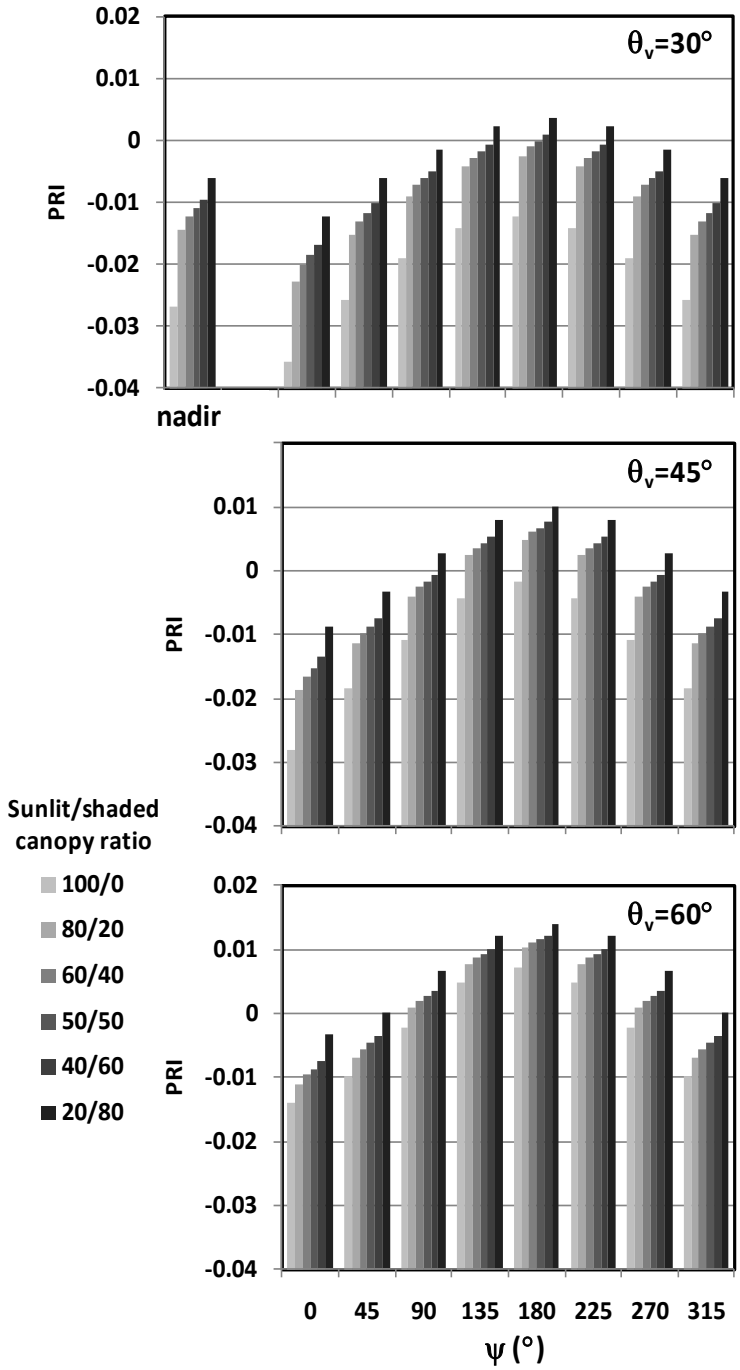

Figure 6. Changes in PRI values when 2-layer simulations were performed with various sunlit/shaded canopy ratios, where the upper layer is sunlit and the lower layer is shaded. Simulations were done using parameters from the mature and green VT canopy, LAI = 2.48 on July 15, 2010. Six sunlit/shaded ratio cases were investigated, as shown in the label, represented by increasingly darker grey tone as more shaded leaves are included. The nadir case is included in the top panel.

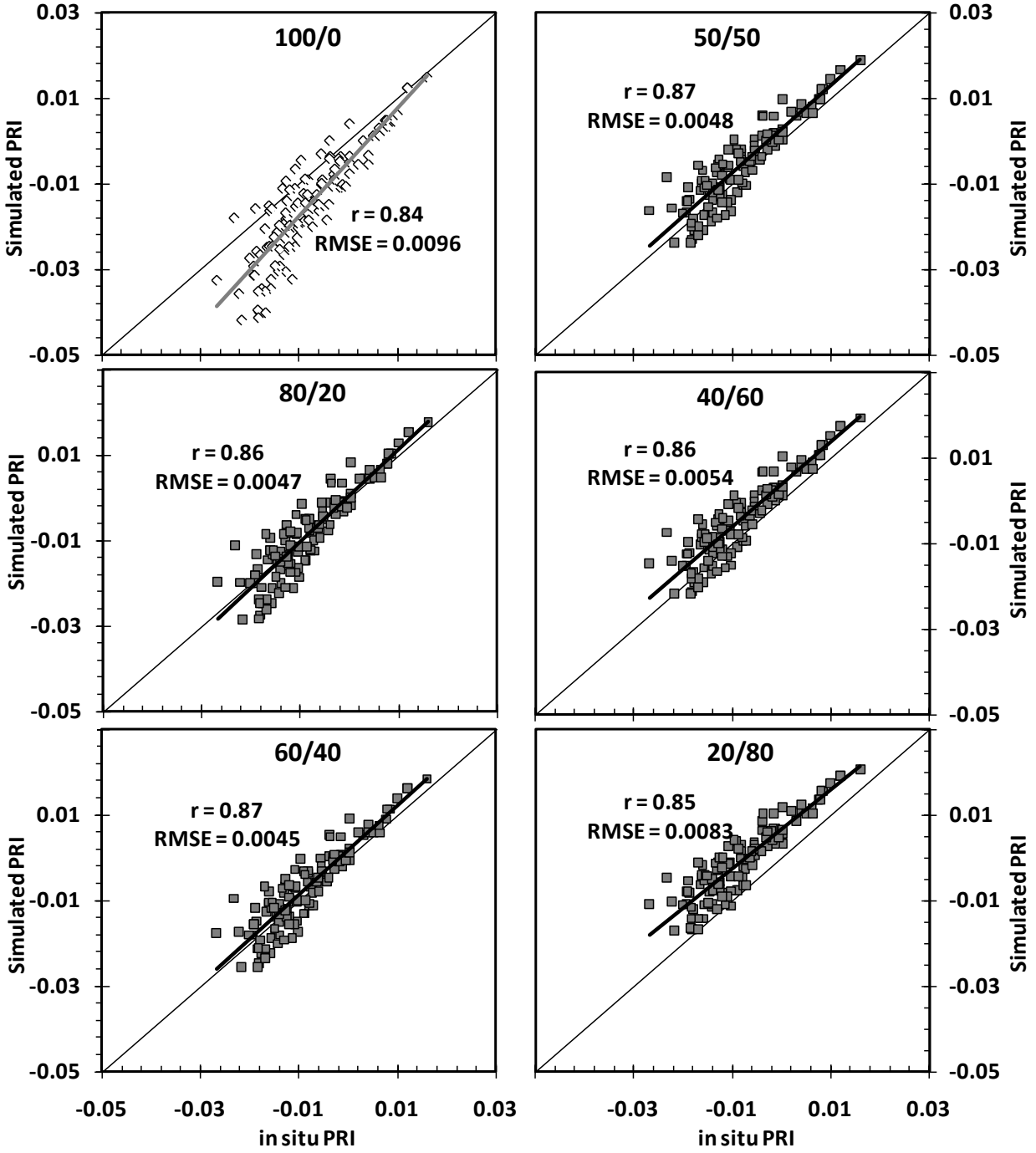

Figure 7. Correlations between *in situ* PRI measurements and PRI values simulated using various sunlit/shaded canopy ratios, for the mature VT canopy on July 15, 2010. LAI = 2.48.

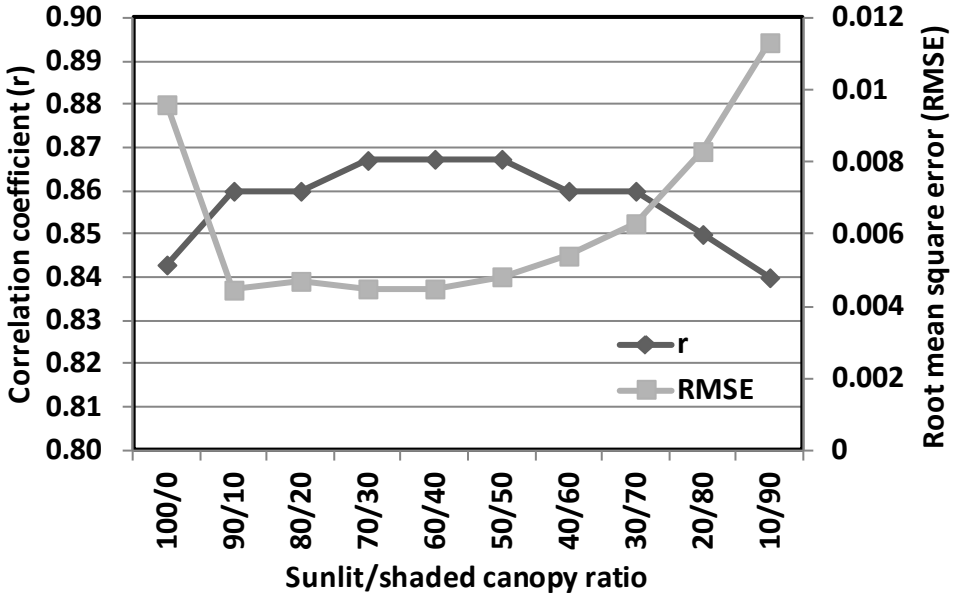

764
765 **Figure 8.** Statistics for the correlation coefficient (r) and root mean square error (RMSE),
766 relating *in situ* PRI measurements and simulated PRI values across various sunlit/shaded canopy
767 ratios. Based on the VT canopy (July 15, 2010; LAI = 2.48).
768

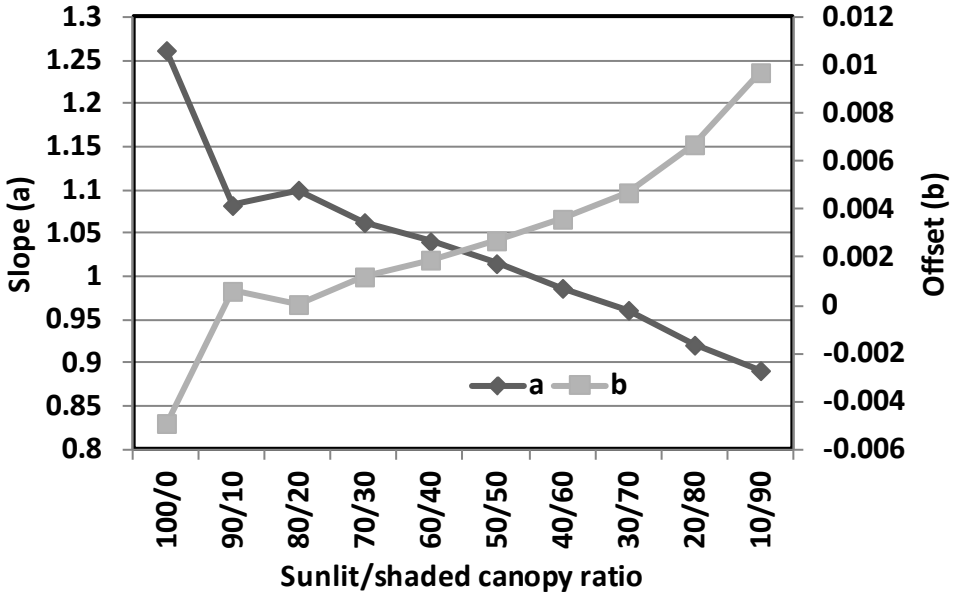

769
770 **Figure 9.** Parameters of the regression line (y=ax+b) relating *in situ* and simulated PRI values,
771 using various sunlit/shaded canopy ratios. Parameter "a" is the slope while "b" is the offset of the
772 regression line. Based on the VT canopy (July 15, 2010; LAI = 2.48).

773 **Table 1.** Value or range of parameters used as input to ACRM in this study.

Date	July 1, 2010	July 15, 2010	August 9, 2010
LAI	1.92	2.48	1.81
Solar zenith angle (θ_s)	16.6° to 42.8°	18.1° to 45.3°	24.1° to 51.2°
View zenith angle (θ_v)	0°, 30°, 45°, 60°		
Relative azimuth angle (ψ)	0° to 315° at 45° increments		
Relative leaf size	0.15		
Markov parameter	1.0		
Leaf angle distribution parameter	$\varepsilon = 0$; $\theta_m = 0$		

774
775
776 **Table 2.** Correlation coefficients (r) and root mean square errors (RMSE) relating *in situ* PRI
777 measurements and ACRM-simulated PRI values using various sunlit/shaded canopy ratios are
778 presented for three additional days: an early 2008 growth stage and two 2010 growth stages.

		100/0	80/20	60/40	50/50	40/60	20/80
August 1, 2008	r	0.71	0.80	0.85	0.86	0.84	0.82
	RMSE	0.019	0.009	0.006	0.004	0.006	0.007
July 1, 2010	r	0.80	0.77	0.78	0.78	0.75	0.68
	RMSE	0.023	0.010	0.007	0.005	0.006	0.007
August 9,2010	r	0.52	0.57	0.62	0.65	0.65	0.64
	RMSE	0.022	0.014	0.010	0.010	0.011	0.012

779
780